The Inhibitor Protein (IF_1) Promotes Dimerization of the Mitochondrial F_1F_0-ATP Synthase†

José J. García,*,‡,§ Edgar Morales-Ríos,‡ Paulina Cortés-Hernández,‡ and José S. Rodríguez-Zavala‡

Departamento de Bioquímica and Cardiovascular Disease's Genomic and Proteomic Study Group, Instituto Nacional de Cardiología Ignacio Chávez, Juan Badiano 1, Col. Sección XVI, México, D.F., Mexico 14080

Received February 17, 2006; Revised Manuscript Received July 28, 2006

ABSTRACT: The effect of increased expression or reconstitution of the mitochondrial inhibitor protein (IF_1) on the dimer/monomer ratio (D/M) of the rat liver and bovine heart F_1F_0-ATP synthase was studied. The 2-fold increased expression of IF_1 in AS-30D hepatoma mitochondria correlated with a 1.4-fold increase in the D/M ratio of the ATP synthase extracted with digitonin as determined by blue native electrophoresis and averaged densitometry analyses. Removal of IF_1 from rat liver or bovine heart submitochondrial particles increased the F_1F_0-ATPase activity and decreased the D/M ratio of the ATP synthase. Reconstitution of recombinant IF_1 into submitochondrial particles devoid of IF_1 inhibited the F_1F_0-ATPase activity by 90% and restored partially the D/M ratio of the whole F_1F_0 complex as revealed by blue native electrophoresis and subsequent SDS−PAGE or glycerol density gradient centrifugation. Thus, the inhibitor protein promotes or stabilizes the dimeric form of the intact F_1F_0-ATP synthase. A possible location of the IF_1 protein in the dimeric structure of the rat liver F_1F_0 complex is proposed. According to crystallographic and electron microscopy analyses, dimeric IF_1 could bridge the F_1-F_1 part of the dimeric F_1F_0-ATP sythase in the inner mitochondrial membrane.

The F_1F_0-ATP synthase of energy-transducing membranes is the smallest and most efficient molecular motor of nature (*1*). During ATP synthesis, proton flow drives the rotation of a ring of 10−12 c subunits of its F_0 proton channel; this is connected to the central stalk and therefore drags the γ subunit whose gyration induces the alternating release of newly synthesized ATP from the three catalytic α/β interfaces of F_1 (*2*, *3*). A peripheral stalk works as a stator by connecting the α and β subunits of the F_1 part to static subunits of F_0 (*4*). This rotational mechanism is completely reversible; when the transmembrane proton gradient decreases, the enzyme becomes an ATPase that rotates in the opposite direction as driven by ATP binding energy (*3*, *5*). To prevent wasteful ATP cleavage, the enzyme is controlled in bacteria, chloroplasts, and mitochondria, albeit by different mechanisms. In mitochondria, this regulation is carried out by a powerful inhibitor of ATP synthesis and hydrolysis of 10 kDa (IF_1)[1] that binds to the soluble F_1 part with a 1:1 stoichiometry (*6*, *7*). As shown by cross-linking studies, IF_1 interferes with rotation of the central stalk and with the conformational changes of the catalytic α/β interfaces by binding at a distance $\leq$12 Å from the α, β (*8*, *9*) catalytic interfaces and the rotary γ and ϵ subunits of F_1 (*10*). This was subsequently confirmed by resolution of the N-terminal inhibitory portion of bovine IF_1 reconstituted into its corresponding F_1-ATPase (*11*) showing that the N-terminal side of IF_1 actually interacts with the γ subunit of the rotor, and it binds in a catalytic α/β interface.

It has also been shown that IF_1 self-associates as an inhibitory dimer (*12*) that induces dimerization of soluble F_1 particles (*13*). Indeed, the crystal form of the F_1I complex containing the reconstituted inhibitory protein exhibits this dimeric structure (*11*). These findings raised the question of the extent to which IF_1 contributes to the dimerization of the native F_1F_0-ATP synthase in mitochondria. In this regard, the effect of removal of IF_1 on the dimer/monomer (D/M) distribution of mitochondrial F_1F_0 extracted with different detergents has been studied, either genetically as in yeast mitochondria (*14*) or physically by releasing IF_1 from bovine heart submitochondrial particles (*15*). In both systems it was shown by blue native electrophoresis (BN-PAGE) that dimeric F_1F_0 is formed even though the preparations lack IF_1. From these and other studies it was shown that, rather than IF_1, other subunits of F_0 such as e and g are essential for F_1F_0 dimerization (*16*−*18*). These studies also showed that the F_1F_0 dimer has a key role in the morphology of the mitochondrial inner membrane and in mtDNA stability,

† This work was supported by Grants J-34744-N and V43814-M from CONACyT, México.

* Address correspondence to this author. Tel: (011-5255) 5573-2911 ext 1298. Fax: (011-5255) 5573-0926. E-mail: jjgarcia_trejo@yahoo.com.

‡ Departamento de Bioquímica, Instituto Nacional de Cardiología Ignacio Chávez.

§ Cardiovascular Disease's Genomic and Proteomic Study Group, Instituto Nacional de Cardiología Ignacio Chávez.

[1] Abbreviations: BN-PAGE, blue native polyacrylamide gel electrophoresis; D/M, ratio of dimeric/monomeric species of the F_1F_0-ATP synthase; EDTA-SMP, submitochondrial particles prepared in the presence of EDTA and lacking IF_1; EM, electron microscopy; F_1-IF_1, soluble F_1-ATPase complexed with its inhibitor protein; IF_1, inhibitor protein of the mitochondrial F_1F_0-ATPase; MF_1F_0, F_1F_0-ATP synthase complex from bovine heart mitochondria; MgATP-SMP, submitochondrial particles prepared in the presence of MgATP containing the endogenous IF_1; OSCP, oligomycin sensitivity conferring protein of F_1F_0-ATP synthase; SMP, submitochondrial particles.

10.1021/bi060339j CCC: $33.50
Published on Web 09/29/2006

because the e and g yeast deletion mutants eventually lose the cristae and the mtDNA (*16*−*18*). However, the effect of mitochondrial IF_1 increased expression or its reconstitution on the D/M ratio of the whole F_1F_0 complex has not been studied in conditions where the active ATP synthase dimer is enriched (*16*, *19*, *20*).

Therefore, we determined the effect of overexpressing or reconstituting IF_1 on the D/M ratio of the mitochondrial or particulate F_1F_0-ATP synthase that was subsequently extracted with digitonin. We used mitochondria from rat liver where the ratio of IF_1/F_1 is 0.4 (*21*) and mitochondria from rat AS-30D hepatoma where this ratio raises to about 1.0 and IF_1 is therefore more efficiently associated to F_1F_0 (*22*). We compared the D/M ratio of the ATP synthase solubilized from hepatoma to that found in normal rat liver mitochondria and submitochondrial particles by BN-PAGE. In addition, we assayed the effect of reconstituting recombinant rat liver IF_1 on the D/M ratio of the rat F_1F_0-ATP synthase solubilized from submitochondrial particles. The results of increased expression and reconstitution of IF_1 are consistent with each other and show that IF_1 participates in the dimerization of the intact mitochondrial F_1F_0-ATP synthase.

MATERIALS AND METHODS

Rat liver and AS-30D hepatoma mitochondria were isolated by differential centrifugation as described before (*22*). Submitochondrial particles containing its endogenous IF_1 (MgATP-SMP) or devoid of IF_1 (EDTA-SMP) were prepared by sonication as described for the bovine heart SMP (*10*). Recombinant rat liver IF_1 was overexpressed from the pMal-IF_1 plasmid and purified by the maltose affinity column described elsewhere (*23*). Alternatively, the recombinant IF_1 from rat liver or bovine heart were overexpressed with the pJSRLIF_1 plasmid or its bovine heart counterpart (pJSBHIF_1), which are derivatives of plasmid pIN-III-A3 (*22*), and purified by ammonium sulfate precipitation followed by carboxy methyl chromatography as described before (*24*).

Most of the chemicals were purchased from Sigma, including ATP, ADP, lauryl maltoside, digitonin, and coupling enzymes for activity assays (pyruvate kinase and lactate dehydrogenase). Reactants for SDS−PAGE and BN-PAGE were obtained from Bio-Rad. Coomassie blue for native gels was purchased from Serva.

Blue Native Electrophoresis of Solubilized Mitochondria and Submitochondrial Particles. BN-PAGE was carried out essentially as described by Schägger and Von Jagow (*25*). Because the detergent/protein ratio is crucial during mitochondrial solubilization, special care was taken in the protein determination procedure. This was carried out by the TCA−Lowry protein assay (*26*) that eliminates any interference from buffer components. In this way, after careful titration of digitonin/protein ratios, an optimal detergent/protein ratio of 1.5 mg of digitonin/mg of protein was found as the best condition to extract intact F_1F_0 in its monomeric and dimeric forms. This ratio was therefore kept constant in all experiments shown. After mitochondrial solubilization, BN-PAGE was carried out in minigel format by overnight 40 V runs at 4 °C using 75−150 μg of solubilized protein per lane. Gels were then fixed and stained with Coomassie or used for 2D SDS−PAGE before fixation as described elsewhere (*10*). Lanes of BN gels that were chosen for 2D SDS−PAGE were excised and incubated for a half hour in 1% SDS and 5 mM DTT before loading them into a 10−22% denaturing gel. When necessary, "in-gel ATPase activity" was developed by incubating BN-PAGE gels in "ATPase developing buffer" (50 mM glycine, 0.15% lead acetate, 7.5 mM $MgCl_2$, and 7.5 mM ATP, pH 8.5) for several hours as indicated.

Alternatively, separation of dimeric and monomeric F_1F_0-ATP synthase was carried out with 20−40% glycerol gradient centrifugations as described before (*27*).

Reconstitution of Recombinant Rat Liver IF_1 into Submitocondrial Particles. Purified recombinant rat liver IF_1 was reconstituted into EDTA-SMP in the presence of 6 mM MgATP as described before (*22*, *23*). The IF_1 reconstituted at the amounts indicated in the figures exerted a maximal inhibition of about 90% of the ATPase activity of EDTA-SMP. After reconstitution, EDTA-SMP were washed once by ultracentrifugation at 45000 rpm for removal of excess IF_1 and resuspended in a loading buffer of BN-PAGE for native electrophoresis. When activity assays were carried out, EDTA-SMP reconstituted with IF_1 were resuspended in 250 mM sucrose and 20 mM Tris-HCl, pH 7.0, and ATPase activity was carried out by the spectrophotometric coupled enzyme assay (*28*) following NADH oxidation at 340 nm.

RESULTS

Rat liver mitochondria have an IF_1/F_1 stoichiometry of 0.4 (*21*) that raises to about 1.0 in rat AS-30D liver hepatoma mitochondria due to an increase in the expression of IF_1 (*22*). Concomitantly, and relative to rat liver, there is a higher association of IF_1 with the F_1F_0 complex in AS-30D hepatoma as shown by cross-linking and ATPase activation assays (*22*). Taking advantage of the AS-30D system, we studied the effect of its 2-fold IF_1 increased expression on the ratio of dimeric and monomeric F_1F_0 complexes (D/M). To this end, rat liver and AS-30D mitochondrial preparations were solubilized with digitonin as detailed in Materials and Methods to extract the monomeric and dimeric ATP synthase (*16*, *20*). BN-PAGE and denaturing 2D analyses showed the presence of extracted monomeric and dimeric F_1F_0 complexes in both preparations with a tendency to increase the D/M ratio in AS-30D mitochondria (Figure 1A). To obtain a D/M ratio that will average the variations obtained by densitometric analyses, several digitonin extracts were obtained from different preparations of liver and AS-30D mitochondria that were subjected to BN-PAGE. Furthermore, to avoid variations in the D/M ratio produced by different protein loads, duplicate lanes of liver or hepatoma in different BN gels were loaded with 75 or 150 μg of protein (see representative gel in Figure 1A). Remarkably, a statistically significant increase in the D/M ratio to a value of 1.61 ± 0.22 ($\pm$SD; $n = 6$) was found in AS-30D mitochondria as compared to 1.17 ± 0.07 ($\pm$SD; $n = 6$) found in rat liver (Figure 2). For comparison, the D/M ratio of mitochondrial F_1F_0 extracted with digitonin from bovine heart mitochondria was determined in the same conditions used for rat liver and hepatoma mitochondria. This ratio showed a higher D/M ratio of 2.7 ± 0.9 ($\pm$SD; $n = 3$) after densitometry analyses of different lanes loaded in three separate BN gels (see two representative lanes labeled as "Bov" in Figure 2A). To confirm this result, we also analyzed the D/M ratio of ATP synthase in the so-called MgATP-SMP that retain the endogenous IF_1 protein

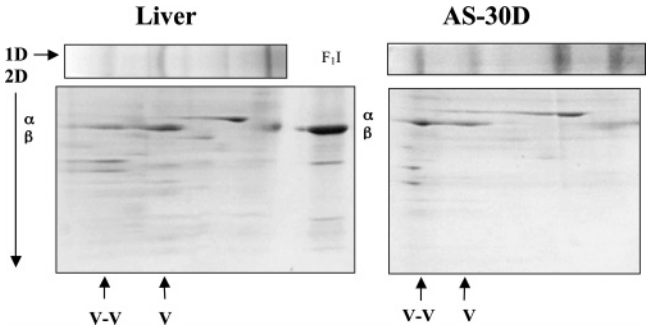

FIGURE 1: Separation of dimeric and monomeric F_1F_0 complexes by BN-PAGE and 2D SDS−PAGE. 150 μg of mitochondrial digitonin extracts of liver (left) or AS-30D (right) were subjected to BN-PAGE (upper horizontal lanes). In the same BN gel, other lanes were loaded with 200 μg of protein of the same samples, excised and subjected to BN-PAGE and subsequently to 2D SDS−PAGE as detailed under Materials and Methods. The two major uppermost bands of BN-PAGE correspond to dimeric (V-V) and monomeric (V) forms of the ATP synthase as resolved by 2D SDS−PAGE. An F_1 standard was included showing the position of the α and β bands of F_1. Other mitochondrial complexes were resolved with higher protein loads; for example, the faint bands above and below the ATP synthase monomer (V) correspond to monomeric complex I and dimeric bc_1 (see also Figure 2A). Other major proteins resolved in the right side of 2D gels were not identified.

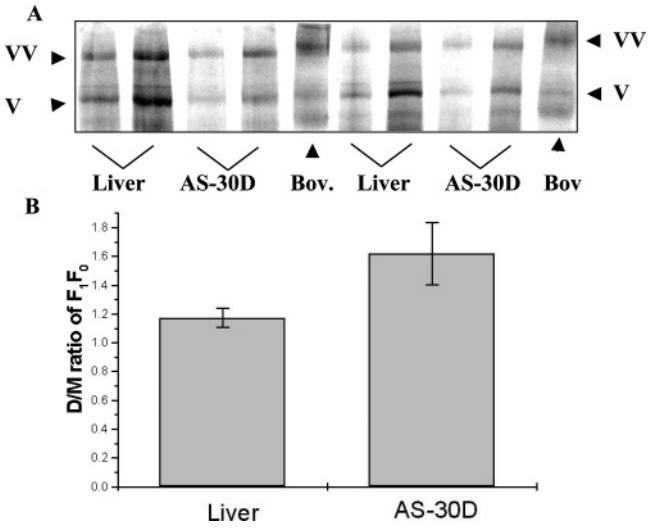

FIGURE 2: Densitometric analyses of the D/M ratio of the F_1F_0-ATP synthase in liver and hepatoma mitochondria. (A) BN-PAGE of digitonin extracts obtained from liver and AS-30D mitochondria were subjected to densitometric analyses to calculate the relative intensities of dimeric (V-V) and monomeric (V) bands. Lanes 1, 3, 5, 6, and 8 were loaded with 75 μg of protein, whereas lanes 2, 4, 7, and 9 were loaded with 150 μg of protein. Lanes labeled as Bov were loaded with 100 μg of digitonin extracts obtained from bovine heart mitochondria. (B) Statistical analyses showed a significant increase of the dimeric F_1F_0 in AS-30D mitochondria compared to rat liver. A Student's *t*-test indicated that the differences between liver and AS-30D samples are statistically significant ($p = 0.00071$, $n = 6$). Error bars indicate the standard deviation of the data. The actual SD values are indicated in the text (see the Results section where this figure is cited).

functionally bound to the F_1F_0-ATP synthase. After solubilizing MgATP-SMP from liver and hepatoma with the same optimal amount of digitonin (1.5 mg/mg of protein), the monomeric (V) and dimeric (V-V) forms of the F_1F_0 complex were resolved by BN-PAGE followed by denaturing 2D SDS−PAGE and Coomassie staining (Figure 3). It was clearly evident that the D/M ratio of F_1F_0 of hepatoma SMP

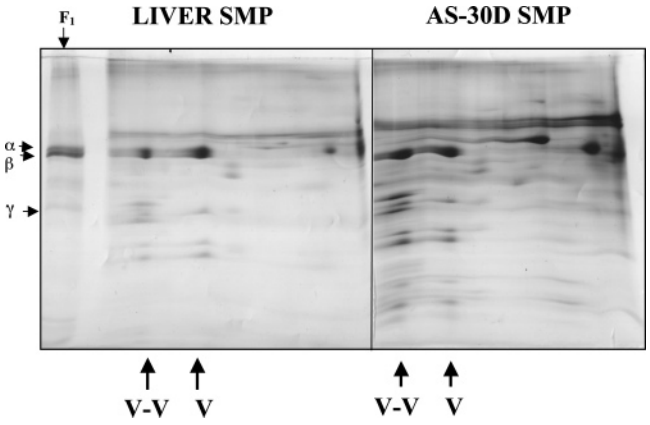

FIGURE 3: 2D SDS−PAGE resolution of dimeric and monomeric F_1F_0 in liver and AS-30D SMP. 150 μg of SMP digitonin extracts were subjected to BN-PAGE (not shown) and 2D SDS−PAGE. The amount of dimeric F_1F_0 (V-V) was increased relative to the monomeric (V) ATP synthase in AS-30D hepatoma SMP, as compared to rat liver SMP. The right side bands that increase in AS-30D were not identified.

was higher than in SMP from normal rat liver. Densitometry analyses of the α/β bands of the F_1F_0 dimer and monomer resolved by 2D SDS−PAGE showed that the D/M ratio of ATP synthase in AS-30D SMP was 0.9 whereas in liver SMP it was 0.6. This result is similar to that found with extracted mitochondria. However, the D/M ratios are lower in SMP, presumably due to disruption of the inner membrane structure through SMP preparation. Figure 3 shows that a couple of proteins resolved just above and below the γ subunit seem to comigrate with the ATP synthase dimer and to increase in AS-30D mitochondria. However, these bands remained in the same position of 2D gels after the ATP synthase dimer was almost completely removed during activation conditions (see below, Figure 4). Thus, these proteins comigrate with the dimer but do not seem to be associated stoichiometrically with it. The increase in other proteins in AS-30D that resolved in the far right side of the 2D gel was not further explored here because those do not form part of the ATP synthase dimer or the monomer. Taken together, the data show that the higher the expression of IF_1, the higher the D/M ratio of the F_1F_0-ATP synthase.

The differences between liver and AS-30D mitochondria are not only limited to the content of IF_1. Other factors such as the lipid composition or the shifts in expression of other mitochondrial proteins (see, for example, Figure 3) might influence the D/M ratio of the ATP synthase. Therefore, to assess the actual role of IF_1 on the control of the ATP synthase dimerization, we modeled the in vivo IF_1 increased expression by in vitro reconstitution of inhibitory amounts of IF_1 into rat liver F_1F_0 of SMP devoid of IF_1. An increase in D/M ATP synthase induced by IF_1 reconstitution would indicate that this protein is a key factor promoting F_1F_0 dimerization. Therefore, rat liver SMP from which most of the endogenous IF_1 was previously released (EDTA-SMP; see Materials and Methods) were reconstituted with several concentrations of recombinant IF_1 that exerted a maximal inhibition of about 90% of the F_1F_0-ATPase activity (Figure 4). EDTA-SMP with or without reconstituted IF_1 (4 μg/50 μg of SMP) were solubilized and analyzed by BN-PAGE and subsequent 2D SDS−PAGE together with a control sample of Mg-ATP SMP containing the endogenous IF_1

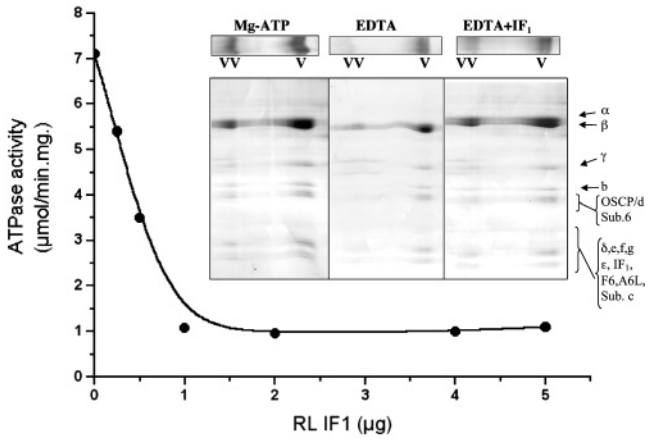

FIGURE 4: Effect of IF_1 reconstitution on the F_1F_0-ATPase activity and the D/M ratio of rat liver submitochondrial particles. 50 μg of EDTA-SMP devoid of IF_1 were incubated with the indicated amounts of recombinant IF_1 as indicated in Materials and Methods. 5 μL aliquots were withdrawn after 15 min to measure the specific ATPase activity spectrophotometrically. About 1 μg of IF_1 was enough to exert maximal ATPase inhibition (86%). Inset: 1D BN-PAGE and 2D SDS−PAGE of SMP extracted with digitonin. Left panel, SMP containing its endogenous IF_1 (MgATP-SMP); center panel, SMP lacking most of its endogenous IF_1 (EDTA-SMP); right panel, SMP-EDTA reconstituted with saturating IF_1 (4 μg of IF_1/50 μg of SMP). The positions of the ATP synthase dimer (V-V) and its monomer (V) are indicated. Removal and reconstitution of IF_1 were carried out as described in Materials and Methods. ATPase activities of MgATP, EDTA, and EDTA-SMP reconstituted with IF_1 were 0.8, 6.5, and 1.1 μmol min^{-1} (mg of protein)$^{-1}$, respectively.

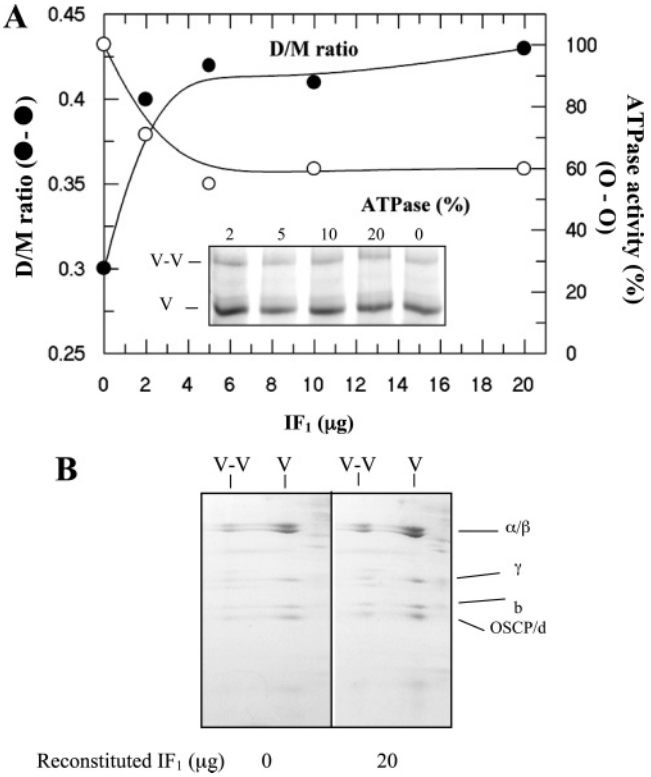

FIGURE 5: Effect of IF_1 reconstitution on the soluble F_1F_0-ATPase activity and the D/M ratio of rat liver digitonin mitochondrial extracts. (A) The indicated amounts of recombinant IF_1 isolated in solubilization buffer were reconstituted as detailed in Materials and Methods into rat liver mitochondrial digitonin extracts containing 115 μg of proteins. Immediately after IF_1 reconstitution, 2−4 μL aliquots containing 15 μg of protein were withdrawn to measure spectrophotometrically the ATPase activity in the presence of digitonin (0.05%). Controls confirmed that 0.05% digitonin did not interfere with coupling enzymes of the assay. The plot shows the average ATPase activity of two independent determinations (○). 100% ATPase activity of control samples incubated in conditions of reconstitution but without IF_1 was 1.3 μmol min^{-1} (mg of protein)$^{-1}$. Following ATPase determination, about 100 μg of all digitonin extracts were loaded into 1D BN-PAGE (inset). The positions of the ATP synthase dimer (V-V) and its monomer (V) are indicated. The amounts of reconstituted IF_1 (0−20 μg) are shown on top of the inset. Average D/M ratios obtained by densitometry intensities of the ATP synthase dimer and monomer bands are plotted (●). (B) Duplicate lanes of the 1D BN-PAGE (inset of panel A) containing about 100 μg of control (no IF_1, left) or reconstituted IF_1 (20 μg, right) were subjected to 2D SDS−PAGE, followed by fixation and Coomassie staining. The positions of the ATP synthase dimer (V-V) and monomer (V) as well as the resolved F_1F_0 subunits are indicated. Densitometry analyses of the α/β intensities indicated an increase in D/M ratio from 0.32 to 0.40, similar to that observed in the BN-PAGE (panel A).

(Figure 4 inset). It was clearly observed that removal of IF_1 decreased the D/M ratio in SMP devoid of IF_1. Furthermore, reconstitution of saturating recombinant IF_1 restored the D/M ratio of the particulate F_1F_0-ATP synthase. To avoid ambiguity of the data due to variations in total protein loaded into the gels, average densitometries of dimeric and monomeric F_1F_0 were carried out with three different 1D and 2D gels loaded with 75 and 150 μg of protein. These analyses showed that the average D/M ratios (±SD) were 0.65 ± 0.04 for MgATP-SMP and 0.17 ± 0.04 in EDTA-SMP; i.e., removal of IF_1 vanished most of the F_1F_0 dimer. Furthermore, when recombinant IF_1 was reconstituted into EDTA-SMP, this ratio was restored to a value of 0.49 ± 0.13. Titration experiments with lower and higher amounts of IF_1 showed that maximal increase in the D/M ratio was attained with saturating inhibitory concentrations of IF_1 (about 2 μg of IF_1/50 μg of SMP). It is important to point out that according to previous studies carried out with the soluble bovine heart F_1-ATPase (*29*) there is no strict correlation between inhibition of ATPase activity and the propensity to form F_1-F_1 dimers as induced by the inhibitor protein; i.e., IF_1 can inhibit almost fully the F_1-ATPase in a mixture of dimeric and monomeric F_1-IF_1 complexes of different D/M ratios that exist in a dynamic equilibrium (*29*). Thus, although higher D/M ratios closer to or higher than 1.0 can be predicted expecting a F_1F_0 dimerization proportional to the 90% inhibition of ATPase activity, the actual D/M ratio can be lower as found here. Keeping this in mind, the recombinant rat liver IF_1 was also reconstituted into the digitonin rat liver mitochondrial extracts obtained with 2.5 mg of detergent/mg of protein to assess the ability of IF_1 to promote dimerization of the soluble F_1F_0. A modest but reproducible increase in the D/M ratio was obtained after 1D BN-PAGE and 2D SDS−PAGE from an average densitometric ratio of 0.30 to a maximal value of 0.43 (Figure 5). Remarkably, the increase in D/M ratio paralleled the decrease in ATPase activity when plotted versus the amount of IF_1 used for reconstitution (Figure 5A). The lower impact of IF_1 on ATPase activity and D/M ratios obtained with extracted F_1F_0 as compared to the particulate ATP synthase (Figure 4) is likely a reflection of inefficient IF_1 binding because it is well described that high salt concentrations (as present in the solubilziation buffer, see Materials and Methods) reduce the yield of IF_1 association to F_1 and F_1F_0. Nevertheless, similar results were obtained when IF_1 was reconstituted into soluble F_1F_0 extracted with

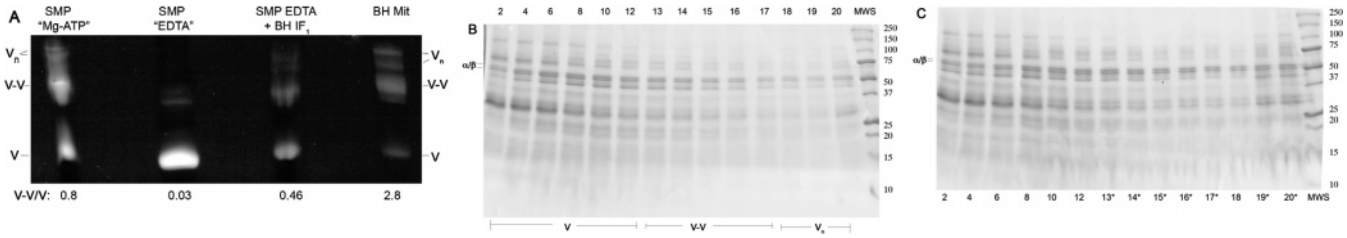

FIGURE 6: Dimerization of bovine heart F_1F_0-ATP synthase induced by reconstitution of recombinant bovine heart IF_1. Three different samples containing 12 mg of MgATP-SMP (1 sample) or EDTA-SMP (2 samples) were diluted to 20 mg of protein/mL in reconstitution buffer. One of the samples containing EDTA-SMP was reconstituted with 2 μg of bovine IF_1/50 μg of SMP as described in Materials and Methods. The other two samples containing MgATP-SMP or EDTA-SMP were incubated in the same conditions but without recombinant IF_1. Subsequently, aliquots of 1.5−3.0 μL were withdrawn from each sample to measure spectrophotometrically the steady-state rate of particulate F_1F_0-ATPase activity. The specific activities obtained were 1.1, 5.4, and 0.53 μmol min^{-1} (mg of protein)$^{-1}$, for MgATP, EDTA, and EDTA + IF_1 SMP, respectively. Afterward, samples were centrifuged once at 186000*g* at 4 °C to remove the reconstitution buffer and the excess IF_1 (if present) by discarding the supernatant. The pellet containing SMP of each sample was resuspended to 15 mg/mL in solubilization buffer and extracted with 2 mg/mL digitonin as described in Materials and Methods. Different aliquots of the digitonin extracts obtained were subjected overnight to 16 h runs of BN-PAGE (A) or 20−40% glycerol density gradient centrifugation at 4 °C (B and C) as described before (*27*). (A) 140 μg of protein from the digitonin extracts of MgATP-SMP (first lane), EDTA-SMP (second lane), and EDTA-SMP reconstituted with bovine heart IF_1 (BH IF_1) (third lane) were loaded on a BN-PAGE gel that was subsequently developed for in-gel ATPase by incubation during 48 h in ATPase developing buffer as described in Materials and Methods. A control lane containing 80 μg of a digitonin extract (1.5 mg/mg of protein) of bovine heart mitochondria was included (fourth lane, BH Mit). Densitometry of the bands of the F_1F_0-ATPase dimer (V-V), monomer (V), and higher F_1F_0 oligomers (V_n) showed the relative percentage of each component as follows: 43% (V-V), 53% (V), and 4% (V_n) for MgATP-SMP; 3% (V-V), 95% (V), and 3% (V_n) for EDTA-SMP; and 32% (V-V), 64% (V), and 4% (V_n) for EDTA-SMP + IF_1. The control lane loaded with the bovine heart mitochondrial extract showed 62% (V-V), 22% (V), and 16% (V_n), similar to the proportions obtained by densitometry of Coomassie staining of BN-PAGE (see Figure 2 and text). The F_1F_0 dimer/monomer ratios (V-V/V) of each sample are indicated at the bottom of the gel. (B, C) 0.5 mL aliquots of the digitonin extract of each SMP sample were subjected to a 16 h run of a 20−40% glycerol gradient centrifugation as described before (*27*). Afterward, each gradient tube was fractionated from top to bottom into 20 fractions of 1 mL each. 15 μL aliquots of selected fractions were loaded on 10−22% gradient SDS−PAGE gels and stained with Coomassie. Gradient separation-obtained digitonin extracts of EDTA-SMP (B) and EDTA-SMP + IF_1 (C) are shown. The regions of the gradients where dimeric (V-V), monomeric (V), and multimeric (V_n) F_1F_0-ATP synthase are enriched are shown at the bottom of panel B. The positions of F_1 α/β bands are indicated, and their intensity shows the relative amount of F_1F_0 on each fraction. Fraction numbers are indicated at the top or at the bottom of each gel. Fractions where the content of dimeric and multimeric F_1F_0-ATP synthase is increased by reconstitution of recombinant bovine IF_1 are labeled with an asterisk. A similar enrichment of dimeric and multimeric bovine heart F_1F_0 at the bottom gradient fractions can be observed with mitochondrial extracts and MgATP-SMP extracts containing its endogenous IF_1. Molecular weight standards (MWS) are shown at the far right of each gel.

digitonin from rat liver SMP (not shown). We next explored more closely the range of 0−2 μg of IF_1 where it induces sharp decreases and increases in ATPase activity and D/M ratio, respectively (Figures 4 and 5). To this end, rat liver MgATP-SMP were reconstituted with 0, 1, and 2 μg of rat liver IF_1, and the D/M ratio of digitonin-extracted F_1F_0 was determined by BN-PAGE and densitometry as before. The average of two independent experiments showed an increase in D/M ratio from 0.45 without reconstituted IF_1 to 0.70 and 0.90 with 1 and 2 μg of IF_1, respectively. These were among the highest D/M ratios obtained after IF_1 reconstitution and likely reflect the IF_1 binding into vacant F_1 sites in SMP. In some experiments, D/M ratios higher than 1 (1.2−1.5) were obtained after reconstitution of 2−4 μg of IF_1/50 μg of SMP (not shown). Taken together, the results show that IF_1 controls the D/M ratio of the whole ATP synthase in the same concentration range at which it does inhibit the ATPase activity of the F_1F_0 complex associated to the inner mitochondrial membrane.

Finally, to confirm the IF_1-promoted F_1F_0 dimerization in other systems and through experimental techniques different to BN-PAGE, bovine heart SMP were subjected to similar reconstitution experiments as those described for rat liver and hepatoma SMP. Besides BN-PAGE, in-gel ATPase activity and parallel glycerol density gradients were carried out with F_1F_0 extracted from bovine heart SMP in order to separate the F_1F_0 dimer from the monomer. MgATP-SMP, EDTA-SMP, and EDTA-SMP reconstituted with 2 μg of IF_1/50 μg of SMP were extracted with digitonin and subjected overnight to BN-PAGE and in parallel to 20−40% glycerol density gradients that separate dimeric from monomeric F_1F_0 extracted from bovine heart mitochondria (*27*). The BN-PAGE gel was also loaded with a control sample of digitonin extract obtained from whole bovine heart mitochondria and developed for in-gel ATPase activity as described in Materials and Methods. This was carried out by incubation of the BN-PAGE gel in ATPase development buffer for 48 h to develop efficiently the residual ATPase activity of samples containing endogenous or reconstituted IF_1. Figure 6A shows that the D/M ratio can be also estimated from the ATPase development of the BN-PAGE gel. As a control, the lane containing the bovine heart mitochondrial extract obtained with 1.5 mg of digitonin/mg of protein showed a densitometric ATPase D/M ratio of 2.8, i.e., very close to the average 2.7 D/M ratio obtained with the densitometry of Coomassie-stained BN-PAGE (see Figure 2). In addition, at least two larger F_1F_0 oligomers (V_n) were also observed representing 9% and 7% of the total functional F_1F_0-ATPase. These F_1F_0 oligomers have been observed before (*30*, *31*). Furthermore, it was also confirmed that ATPase development was proportional to the steady-state F_1F_0-ATPase activity that was measured spectrophotometrically with an ATP regenerating system (see Materials and Methods). The respective steady-state ATPase activities of MgATP-SMP, EDTA-SMP, and EDTA-SMP reconstituted with IF_1 were 1.1, 5.4, and 0.53 μmol min^{-1} (mg of protein)$^{-1}$ as determined immediately after incubation of SMP with or without IF_1. As shown in Figure 6A, the development of ATPase activity in the BN-PAGE correlated with the IF_1 content of SMP; i.e, it was higher for EDTA-SMP, intermediate for MgATP-

SMP, and lower for EDTA-SMP reconstituted with IF_1. Finally, the BN-PAGE combined with ATPase development and densitometry showed clearly that the D/M ratio decreased from 2.8 in the bovine heart mitochondrial extract to 0.81 in MgATP-SMP. This ratio decreased dramatically to 0.03 after removal of IF_1 in EDTA-SMP (concomitant to an increase in ATPase activity of the F_1F_0 monomer), and reconstitution of IF_1 brought a partial recovery of the D/M ratio to 0.5 with an overall decrease in ATPase activity. In addition, it was observed that IF_1 reconstitution also induced the recovery of ATP synthase oligomers larger than the dimer (V_n in Figure 6A). On the other hand, fractionation of the glycerol gradients and subsequent SDS−PAGE showed similar results in that in comparison to EDTA-SMP (Figure 6B), reconstitution of IF_1 into these particles increased the F_1F_0 content in fractions 13−20 where the F_1F_0 dimer and higher ATP synthase oligomers were enriched (Figure 6C). A similar but higher enrichment of the dimer and higher oligomers was also observed in gradients carried out with digitonin extracts from bovine heart mitochondria or MgATP-SMP containing the endogenous IF_1 (not shown; see also ref *27*). No densitometry calculations of D/M ratios were obtained from these gradients because the fractions are not continuous in the gels (Figure 6B,C); however, good D/M estimations were obtained from Figure 6A. In conclusion, the inhibitory protein promotes dimerization of the mitochondrial F_1F_0-ATP synthase from mitochondria of different higher eukaryots, and it also promotes its polymerization to form higher ATP synthase oligomers. However, no strict correlation exists between maximal inhibition by IF_1 and maximal yield of F_1F_0 dimerization. This is likely because other protein factors different from IF_1 are essential for F_1F_0 dimerization and polymerization in the inner mitochondrial membrane.

DISCUSSION

The salient result of this work is that the increased expression or the reconstitution of the inhibitory protein (IF_1) increases the D/M ratio of the mitochondrial F_1F_0-ATP synthase in whole mitochondria and in submitochondrial particles. Therefore, our overall results show that IF_1 promotes and/or stabilizes the dimeric structure of the F_1F_0 complex. These results are in apparent contrast with previous studies showing that genetic or physical removal of IF_1 in yeast mitochondria and bovine SMPs, respectively, does not prevent ATP synthase dimerization (*14*, *15*). However, the prevalence of the F_1F_0 dimer as formed through F_0 interactions by other subunits such as e or g in the absence of IF_1 (*14*) does not discard a possible role of IF_1 on the formation or stabilization of the F_1F_0 dimer through F_1-F_1 bridging. By studying the effect of increased expression or reconstitution of IF_1, we used two alternative approaches that together with statistical averages of densitometry analyses of BN-PAGE and 2D SDS−PAGE complement each other to support the same conclusion: the inhibitory IF_1 binding contributes to the formation of the F_1F_0 dimer. Rat liver and AS-30D hepatoma offer a unique comparative system to assay the effect of IF_1 increased expression in whole mitochondria, because IF_1 is substoichiometric in relation to F_1 in rat liver (*21*). Thus, the effect of a 2-fold IF_1 increased expression as in AS-30D hepatoma on the aggregation state of the mitochondrial F_1F_0-ATP synthase was comparatively assessed with rat liver mitochondria. Furthermore, by modeling the IF_1 increased expression with reconstitution of the recombinant IF_1 on SMP devoid of IF_1, we confirmed the role of IF_1 in promoting the dimerization of the whole ATP synthase associated to the inner mitochondrial membrane. A similar reconstitution experiment carried out with the bovine IF_1 and SMP showed no changes in the D/M ratio of the ATP synthase extracted with Triton X-100 (*15*). Because the dimeric ATP synthase extracted with Triton X-100 is less enriched and inactive (*15*), compared to that obtained with digitonin, which is highly enriched and functional as ATPase (see Figure 6A and refs *19* and *27*), we consider that the dimeric ATP synthase extracted with digitonin is structurally and functionally a better model to study the changes in the D/M ratio of the ATP synthase dimer. In this regard, we have also observed oligomycin sensitivity and IF_1-increased D/M ratio on the digitonin-extracted and sucrose gradient-purified bovine F_1F_0 (see Figure 6B,C), together with an IF_1 increase in D/M ratio of lauryl maltoside-extracted F_1F_0 from rat liver mitochondria (not shown). Besides, restoration of the D/M ratio by reconstitution of exogenous IF_1 after removal of the endogenous IF_1 in EDTA-SMP (Figures 4−6) discards a significant instability or irreversible denaturation of the F_1F_0 dimer or monomer caused by the activation conditions used to release IF_1 from SMP; otherwise, restoration of the D/M ratio by IF_1 would not be observed. Furthermore, the finding that recombinant IF_1 also increases the D/M ratio of the digitonin-extracted ATP synthase in negative parallelism with a partial inhibition of the F_1F_0-ATPase activity (Figure 5) confirms that IF_1 promotes or stabilizes the dimeric F_1F_0 structure. Nevertheless, the lower impact of IF_1 on the D/M ratio and on ATPase activity of soluble F_1F_0 as compared with its effects in SMP indicates that IF_1 is less efficiently reconstituted to soluble F_1F_0 in the solubilization media than in SMP. This might be related to the high salt concentrations (EACA and Tris) in the solubilization buffer that are known to decrease IF_1 binding to F_1F_0. However, this also suggests that IF_1 is more efficient to promote or stabilize the F_1F_0 dimer when it is integrated in the inner mitochondrial membrane than when it is solubilized in digitonin micelles. Finally, the promotion of F_1F_0 dimerization by IF_1 was also confirmed in the bovine heart mitochondrial system. Removal and reconstitution of bovine IF_1 from and into SMP controlled dimerzation and even higher order oligomerization of the bovine F_1F_0 (Figure 6). This was confirmed by developing of ATPase activity in the BN-PAGE gel (Figure 6A) and by enrichment of dimeric and multimeric F_1F_0 in the bottom fractions of glycerol density gradients carried out after reconstitution of IF_1 into EDTA-SMP (Figure 6B,C). Thus, the role of IF_1 in the dimerization of F_1F_0 is not exclusive of rat liver, but it is extended into bovine heart mitochondria, and we also have evidence that the same effect of IF_1 occurs in human mitochondria from cultured cells (Cortés-Hernández et al., submitted for publication). It seems therefore that the high propensity to dimerize of IF_1 from mitochondria of higher eukaryots is the key factor that lacks the yeast IF_1 to contribute in the dimerization of the whole F_1F_0 in yeast mitochondria.

On the other hand, the present results showing that IF_1 contributes to F_1F_0 dimerization are consistent with a number

of structural and biophysical studies. It is well documented that IF_1 adds stability to the soluble F_1 and to the whole ATP synthase in SMP to denaturants and high pressure (*32*, 33). This is also in consonance with the observed IF_1-induced dimerization of the soluble F_1 (*13*, *29*). Therefore, a structure similar to that of the soluble F_1I dimer could exist in the whole dimeric F_1F_0 of the inner mitochondrial membrane. The location of IF_1 on the native structure of the F_1F_0-ATP synthase molecule is an unresolved issue that has been studied for several decades. Cross-linking (*8*−*10*) and subsequent crystallographic analyses (*11*) have shown that IF_1 binds in a cleft formed by an α/β interface and the γ subunit, thus hindering catalytic conformational changes as well as rotary motions of the central stalk (*10*, *11*). On the other hand, the C-terminal sides of two IF_1s form a coiled coil structure that is instrumental in the dimerization of two soluble F_1 molecules bound to their N-termini. Our results indicate that, in order to stabilize the dimeric structure of the whole F_1F_0 molecule, IF_1 must form a bridge between both extramembranal F_1 parts. Recently, we resolved the structure of the dimeric F_1F_0-ATP synthase from bovine heart mitochondria by high-resolution electron microscopy (EM) (*27*). It is relevant that the MF_1F_0 dimer showed a crossed bridging protein density between the two F_1 moieties which is reminiscent of the IF_1 bridge found in the crystal structure of the F_1-I complex (*11*).

On the basis of these cross-linking, crystallographic, and EM antecedents together with our present data, the approximate position of the IF_1 bridge in the whole rat liver F_1F_0 is proposed in Figure 7. According to a previous model of monomeric F_1F_0 (*34*), the location of IF_1 in the dimer interface was modeled by simple fitting of the crystal structure of rat liver F_1-ATPase (*35*) with a model of the rat liver IF_1 constructed with the software SWISS-MODEL according to the coordinates of the bovine IF_1 (*36*). A bent conformer of the four crystallographic bovine IF_1 structures (*36*) was used to form a crossed IF_1 dimer in the F_1F_0 dimer interface. Using RASMOL 2.6, the inhibitory N-terminal IF_1 sides were oriented close to the rotor/stator interfaces between α/β and γ/ϵ subunits, whereas the C-terminal sides were bent upward close to the position of the OSCP subunits according to cross-linking and crystallographic studies (*10*, *11*). To accommodate the two IF_1 molecules in a F_1-F_1 distance of about 10 Å as observed in the bovine F_1F_0 dimer (*27*), IF_1 bending was necessary to reduce the observed 62 Å that separate the extended structure of the IF_1 dimer (*11*). In the present model, the C-terminal sides of both IF_1s are proposed to cross the interface and interact with the OSCP subunit of the neighboring monomer. Crossed protein structures have been observed in the bovine heart IF_1 crystal (*36*) and in the iron sulfur protein (ISP) of the dimeric bc_1 respiratory complex III (*37*). However, in the bc_1 complex the bridging protein ISP induces crossed-electron transfer (*38*, *39*). In contrast, in this proposed position, the IF_1 protein would have a better resistance to the rotational drag of the central rotor, which is one of its conformational targets for inhibition (*27*). Thus, this working model explains how IF_1 can stabilize the F_1F_0 dimer, and reciprocally, the dimeric F_1F_0 will reinforce the inhibitory function of IF_1. The exact position of IF_1 in the dimeric F_1F_0 will wait for further structural analyses of higher resolution. Our conic working model of the rat liver F_1F_0 dimer was constructed according to the EM structure of the dimeric bovine heart F_1F_0 (*27*) assuming a 1:1 stiochiometry of IF_1 per F_1F_0 in the ATP synthase dimer, as found in soluble F_1-I and monomeric F_1F_0-I complexes; however, the exact stiochiometry remains to be determined. The model does not exclude that other second stalk subunits presumably located in the dimer interface (*27*) (not shown) would also contribute to the observed F_1-F_1 crossing bridge. In this dimer, the close F_0-F_0 interface is likely formed by dimerizing subunits e and g, together with another F_0-F_0 bridging protein of unknown composition (?) that lies on the intermembrane space side (see Figure 7).

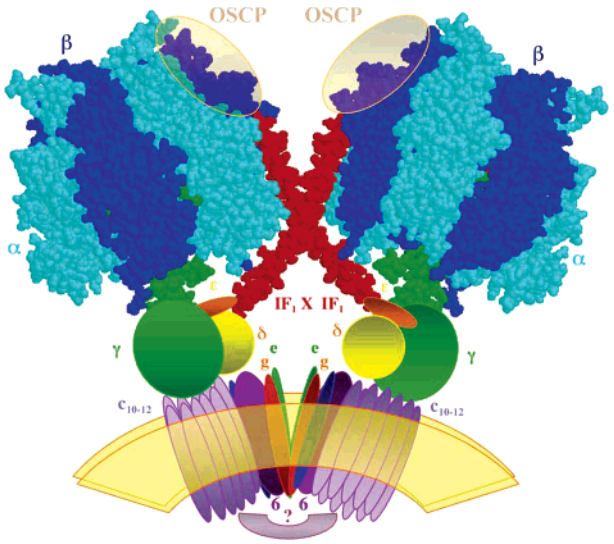

FIGURE 7: Working model of the possible accommodation of the IF_1 bridge on the rat liver dimeric F_1F_0. A structural model of rat liver IF_1 was obtained from a bent conformer of the four resolved for bovine heart IF_1 (*36*). The model was obtained with the software SWISSMODEL (*42*−*44*). Two identical rat liver IF_1 molecules were fitted manually into the F_1-F_1 interface by using RASMOL 2.6. The overall model was made according to the EM structure of bovine heart F_1F_0 that shows a crossing F_1-F_1 bridge in the dimer interface attributable at least in part to IF_1 (*27*). Distances and orientations are approximate, and the possible accommodation of dimerizing subunits e and g in the F_0-F_0 interface is shown. Another F_0-F_0 bridging structure (?) of unknown composition observed in the bovine heart dimer (*27*) was also depicted on the intermembrane space side. The C-terminal sides of both IF_1s are proposed to bend and cross the dimer interface to contact the subunit OSCP, as observed by cross-linking results (*45*, *46*). Peripheral stalk subunits are not shown for simplicity; they are likely to form part of the dimer interface (*27*). Subunits are named according to their respective color; the dark blue F_0 subunit close to subunit 6 is subunit A6L. See text for further details.

Finally, it has recently been shown that an important role of F_1F_0 dimerization is to induce the formation of the inner membrane cristae of mitochondria. Mutations that disrupt the dimeric structure of the ATP synthase shift the shape of the inner mitochondrial membrane from the normal cristae into several concentric layers within enlarged "onion-like" mitochondria (*17*, *30*, *31*, *40*). Thus, the dimeric conic structure of F_1F_0 is a primary building block that polymerizes to form an arc in a budding inner membrane which eventually forms tubular cristae wrapped by a helical F_1F_0 polymer (*41*). By bridging the F_1F_0 dimer, IF_1 should also add stability to the formation of mitochondrial cristae. Experiments are under way in our laboratory to assess the possible role of IF_1 in the stability of the ATP synthase dimer that gives shape to mitochondrial cristae of transfected cells and to confirm the

identity of the F_1-F_1 bridge of the bovine heart F_1F_0-ATP synthase dimer.

ACKNOWLEDGMENT

The valuable suggestions of Prof. Armando Gómez Puyou from the National University of México (UNAM) on the initial manuscript are gratefully acknowledged. The technical assistance of Concepción Bravo and Fernando Minauro-Sanmiguel in the initial part of this work is also acknowledged. The cloned gene of bovine heart IF_1 was a generous gift of Prof. John E. Walker (Medical Research Council, Cambridge, U.K.). The cloned gene of rat liver IF_1 was derived from the pMal-IF_1 plasmid that was a generous gift of Prof. Roderick A. Capaldi (University of Oregon), and it was originally constructed and generously gifted by Prof. Peter L. Pedersen (The Johns Hopkins University, Baltimore).

REFERENCES

1. Noji, H., and Yoshida, M. (2001) The rotary machine in the cell, ATP synthase, *J. Biol. Chem. 276*, 1665−1668.
2. Boyer, P. D. (2002) Catalytic site occupancy during ATP synthase catalysis, *FEBS Lett. 512*, 29−32.
3. Garcia, J. J. (2000) *The F_0F_1-ATP synthase: binding energy, coupling and rotational catalysis*, Vol. 1, 1st ed., Transworld Research Network, Trivandrum.
4. Wilkens, S., and Capaldi, R. A. (1998) Electron microscopic evidence of two stalks linking the F_1 and F_0 parts of the *Escherichia coli* ATP synthase, *Biochim. Biophys. Acta 1365*, 93−97.
5. Garcia, J. J., and Capaldi, R. A. (1998) Unisite catalysis without rotation of the gamma-epsilon domain in *Escherichia coli* F_1-ATPase, *J. Biol. Chem. 273*, 15940−15945.
6. Klein, G., Satre, M., Dianoux, A. C., and Vignais, P. V. (1981) Photoaffinity labeling of mitochondrial adenosine triphosphatase by an azido derivative of the natural adenosine triphosphate inhibitor, *Biochemistry 20*, 1339−1344.
7. Hashimoto, T., Negawa, Y., and Tagawa, K. (1981) Binding of intrinsic ATPase inhibitor to mitochondrial ATPase−stoichiometry of binding of nucleotides, inhibitor, and enzyme, *J. Biochem. (Tokyo) 90*, 1151−1157.
8. Jackson, P. J., and Harris, D. A. (1988) The mitochondrial ATP synthase inhibitor protein binds near the C-terminus of the F_1 beta-subunit, *FEBS Lett. 229*, 224−228.
9. Mimura, H., Hashimoto, T., Yoshida, Y., Ichikawa, N., and Tagawa, K. (1993) Binding of an intrinsic ATPase inhibitor to the interface between alpha- and beta-subunits of F_1F_oATPase upon de-energization of mitochondria, *J. Biochem. (Tokyo) 113*, 350−354.
10. Minauro-Sanmiguel, F., Bravo, C., and Garcia, J. J. (2002) Cross-linking of the endogenous inhibitor protein (IF_1) with rotor (gamma, epsilon) and stator (alpha) subunits of the mitochondrial ATP synthase, *J. Bioenerg. Biomembr. 34*, 433−443.
11. Cabezon, E., Montgomery, M. G., Leslie, A. G., and Walker, J. E. (2003) The structure of bovine F_1-ATPase in complex with its regulatory protein IF_1, *Nat. Struct. Biol. 10*, 744−750.
12. Cabezon, E., Butler, P. J., Runswick, M. J., and Walker, J. E. (2000) Modulation of the oligomerization state of the bovine F1-ATPase inhibitor protein, IF_1, by pH, *J. Biol. Chem. 275*, 25460−25464.
13. Cabezon, E., Arechaga, I., Jonathan, P., Butler, G., and Walker, J. E. (2000) Dimerization of bovine F_1-ATPase by binding the inhibitor protein, IF_1, *J. Biol. Chem. 275*, 28353−28355.
14. Dienhart, M., Pfeiffer, K., Schagger, H., and Stuart, R. A. (2002) Formation of the yeast F1F0-ATP synthase dimeric complex does not require the ATPase inhibitor protein, Inh1, *J. Biol. Chem. 277*, 39289−39295.
15. Tomasetig, L., Di Pancrazio, F., Harris, D. A., Mavelli, I., and Lippe, G. (2002) Dimerization of F_0F_1ATP synthase from bovine heart is independent from the binding of the inhibitor protein IF_1, *Biochim. Biophys. Acta 1556*, 133−141.
16. Arnold, I., Pfeiffer, K., Neupert, W., Stuart, R. A., and Schagger, H. (1998) Yeast mitochondrial F_1F_0-ATP synthase exists as a dimer: identification of three dimer-specific subunits, *EMBO J. 17*, 7170−7178.
17. Arselin, G., Giraud, M. F., Dautant, A., Vaillier, J., Brethes, D., Coulary-Salin, B., Schaeffer, J., and Velours, J. (2003) The GxxxG motif of the transmembrane domain of subunit e is involved in the dimerization/oligomerization of the yeast ATP synthase complex in the mitochondrial membrane, *Eur. J. Biochem. 270*, 1875−1884.
18. Bustos, D. M., and Velours, J. (2005) The modification of the conserved GXXXG motif of the membrane-spanning segment of subunit g destabilizes the supramolecular species of yeast ATP synthase, *J. Biol. Chem. 280*, 29004−29010.
19. Krause, F., Reifschneider, N. H., Goto, S., and Dencher, N. A. (2005) Active oligomeric ATP synthases in mammalian mitochondria, *Biochem. Biophys. Res. Commun. 329*, 583−590.
20. Schagger, H. (2002) Respiratory chain supercomplexes of mitochondria and bacteria, *Biochim. Biophys. Acta 1555*, 154−159.
21. Schwerzmann, K., Hullihen, J., and Pedersen, P. L. (1982) Proton adenosine triphosphatase complex of rat liver mitochondria. Interaction with the ATPase inhibitor peptide covalently labeled with *N*-hydroxysuccinimidyl-*p*-azidobenzoate, *J. Biol. Chem. 257*, 9555−9560.
22. Bravo, C., Minauro-Sanmiguel, F., Morales-Rios, E., Rodriguez-Zavala, J. S., and Garcia, J. J. (2004) Overexpression of the inhibitor protein IF(1) in AS-30D hepatoma produces a higher association with mitochondrial F(1)F(0) ATP synthase compared to normal rat liver: functional and cross-linking studies, *J. Bioenerg. Biomembr. 36*, 257−264.
23. Lebowitz, M. S., and Pedersen, P. L. (1993) Regulation of the mitochondrial ATP synthase/ATPase complex: cDNA cloning, sequence, overexpression, and secondary structural characterization of a functional protein inhibitor,. *Arch. Biochem. Biophys. 301*, 64−70.
24. Van Heeke, G., Deforce, L., Schnizer, R. A., Shaw, R., Couton, J. M., Shaw, G., Song, P. S., and Schuster, S. M. (1993) Recombinant bovine heart mitochondrial F1-ATPase inhibitor protein: overproduction in *Escherichia coli*, purification, and structural studies, *Biochemistry 32*, 10140−10149.
25. Schagger, H., and von Jagow, G. (1991) Blue native electrophoresis for isolation of membrane protein complexes in enzymatically active form, *Anal. Biochem. 199*, 223−231.
26. Peterson, G. L. (1977) A simplification of the protein assay method of Lowry et al. which is more generally applicable, *Anal. Biochem. 83*, 346−356.
27. Minauro-Sanmiguel, F., Wilkens, S., and Garcia, J. J. (2005) Structure of dimeric mitochondrial ATP synthase: novel F0 bridging features and the structural basis of mitochondrial cristae biogenesis, *Proc. Natl. Acad. Sci. U.S.A. 102*, 12356−12358.
28. Garcia, J. J., Tuena de Gomez-Puyou, M., and Gomez-Puyou, A. (1995) Inhibition by trifluoperazine of ATP synthesis and hydrolysis by particulate and soluble mitochondrial F_1: competition with H_2PO_4, *J. Bioenerg. Biomembr. 27*, 127−136.
29. Dominguez-Ramirez, L., Mendoza-Hernandez, G., Carabez-Trejo, A., Gomez-Puyou, A., and Tuena de Gomez-Puyou, M. (2001) Equilibrium between monomeric and dimeric mitochondrial F_1-inhibitor protein complexes, *FEBS Lett. 507*, 191−194.
30. Paumard, P., Vaillier, J., Coulary, B., Schaeffer, J., Soubannier, V., Mueller, D. M., Brethes, D., di Rago, J. P., and Velours, J. (2002) The ATP synthase is involved in generating mitochondrial cristae morphology, *EMBO J. 21*, 221−230.
31. Gavin, P. D., Prescott, M., Luff, S. E., and Devenish, R. J. (2004) Cross-linking ATP synthase complexes in vivo eliminates mitochondrial cristae, *J. Cell Sci. 117*, 2333−2343.
32. de Gomez-Puyou, M. T., Dominguez-Ramirez, L., Perez-Hernandez, G., and Gomez-Puyou, A. (2005) Effect of denaturants on multisite and unisite ATP hydrolysis by bovine heart submitochondrial particles with and without inhibitor protein, *Arch. Biochem. Biophys. 439*, 129−137.
33. Fornells, L. A., Guimaraes-Motta, H., Nehme, J. S., Martins, O. B., and Silva, J. L. (1998) Pressure effects on the interaction between natural inhibitor protein and mitochondrial F_1-ATPase, *Arch. Biochem. Biophys. 349*, 304−312.
34. García, J. J., Minauro-Sanmiguel, F., and Bravo, C. (2002) in *Recent Research Developments in Human Mitochondrial Myopathies* (Garcia, J. J., Ed.) p 21, Research Signpost, Trivandrum.

35. Bianchet, M. A., Hullihen, J., Pedersen, P. L., and Amzel, L. M. (1998) The 2.8-Å structure of rat liver F_1-ATPase: configuration of a critical intermediate in ATP synthesis/hydrolysis, *Proc. Natl. Acad. Sci. U.S.A. 95*, 11065−11070.
36. Cabezon, E., Runswick, M. J., Leslie, A. G., and Walker, J. E. (2001) The structure of bovine IF(1), the regulatory subunit of mitochondrial F-ATPase, *EMBO J. 20*, 6990−6996.
37. Iwata, S., Lee, J. W., Okada, K., Lee, J. K., Iwata, M., Rasmussen, B., Link, T. A., Ramaswamy, S., and Jap, B. K. (1998) Complete structure of the 11-subunit bovine mitochondrial cytochrome bc1 complex, *Science 281*, 64−71.
38. Gutierrez-Cirlos, E. B., and Trumpower, B. L. (2002) Inhibitory analogs of ubiquinol act anti-cooperatively on the yeast cytochrome bc_1 complex. Evidence for an alternating, half-of-the-sites mechanism of ubiquinol oxidation, *J. Biol. Chem. 277*, 1195−1202.
39. Covian, R., Gutierrez-Cirlos, E. B., and Trumpower, B. L. (2004) Anti-cooperative oxidation of ubiquinol by the yeast cytochrome bc_1 complex, *J. Biol. Chem. 279*, 15040−15049.
40. Arselin, G., Vaillier, J., Salin, B., Schaeffer, J., Giraud, M. F., Dautant, A., Brethes, D., and Velours, J. (2004) The modulation in subunits e and g amounts of yeast ATP synthase modifies mitochondrial cristae morphology, *J. Biol. Chem. 279*, 40392−40399.
41. Allen, R. D. (1995) Membrane tubulation and proton pumps, *Protoplasma 189*, 1−8.
42. Schwede, T., Kopp, J., Guex, N., and Peitsch, M. C. (2003) SWISS-MODEL: An automated protein homology-modeling server, *Nucleic Acids Res. 31*, 3381−3385.
43. Guex, N., and Peitsch, M. C. (1997) SWISS-MODEL and the Swiss-PdbViewer: an environment for comparative protein modeling, *Electrophoresis 18*, 2714−2723.
44. Peitsch, M. (1995) Protein modeling by E-mail, *Bio/Technology 13*, 658−660.
45. Zanotti, F., Raho, G., Gaballo, A., and Papa, S. (2004) Inhibitory and anchoring domains in the ATPase inhibitor protein IF1 of bovine heart mitochondrial ATP synthase, *J. Bioenerg. Biomembr. 36*, 447−457.
46. Papa, S., Zanotti, F., and Gaballo, A. (2000) The structural and functional connection between the catalytic and proton translocating sectors of the mitochondrial F1F0-ATP synthase, *J. Bioenerg. Biomembr. 32*, 401−411.

BI060339J